Applied Thermal Engineering 253 (2024) 123718

Contents lists available at ScienceDirect

Applied Thermal Engineering

journal homepage: www.elsevier.com/locate/ate

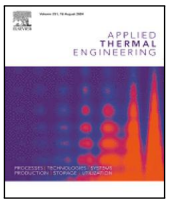

Research Paper

A comparative study on predicting wet cooling tower performance in combined cooling systems for heat rejection in CSP plants

P. Navarro [a], J.M. Serrano [b], L. Roca [b], P. Palenzuela [b], M. Lucas [c], J. Ruiz [c,*]

[a] Departamento de Ingeniería Térmica y de Fluidos, Universidad Politécnica de Cartagena, Dr. Fleming, s/n, 30202 Cartagena, Spain
[b] CIEMAT-Plataforma Solar de Almería-CIESOL, Ctra. de Senés s/n, 04200 Tabernas, Almería, Spain
[c] Instituto de Investigación en Ingeniería de Elche, Universidad Miguel Hernández, Avda. de la Universidad, s/n, 03202 Elche, Spain

ARTICLE INFO

Keywords:
Cooling tower
Thermal performance
Poppe
Merkel
Concentrated solar power
Combined cooling systems

ABSTRACT

Combined Cooling Systems constitute a promising strategy to reduce water consumption in Concentrated Solar Power plants. This paper addresses the comparative evaluation of two different theories based on physical equations (Poppe and Merkel) and three correlations, including a novel and unreferenced one, to predict the performance and water consumption of a wet cooling tower for heat rejection in Concentrated Solar Power plants.

Sixteen sets of experiments were conducted in a fully instrumented pilot plant of combined cooling systems to assess the thermal performance of the cooling tower. Key findings indicate accurate prediction of cooling tower outlet water temperature by both Poppe and Merkel theories, as well as the three correlations, with minimal differences, less than 0.94 °C (2.78%), corresponding to values of R^2 = 0.9918 and RMSE = 0.4650.

When considering all key variables for CSP performance, the three correlations under comparison exhibited comparable prediction accuracy. This study recommends the combination of the Poppe theory with the correlation $\dot{m}_w$ and $\dot{m}_a$, which accounts for air and water mass flow rates independently. This combination demonstrated reasonable accuracy in predicting the outlet water temperature and the water consumption, with average differences of 0.14 °C and 0.01 kg s^{-1}, respectively. These differences correspond to percentage variations of 0.91% and 9.21% for the previously mentioned variables.

This study provides valuable insights for the modelling and analysis of combined cooling systems integrated in CSP plants, advancing beyond previous efforts in the literature.

1. Introduction

According to the climate bulletins issued by Copernicus, the European Union's Earth observation programme, the global surface air temperature in July 2023 was the highest on record for any month in the hourly data on single levels dataset, going back to 1940. July was around 1.5 °C warmer than the 1850–1900 average, the limit established by the Paris Agreement. Numerous regions in the Northern Hemisphere faced severe heatwaves, yet the Southern Hemisphere did not escape this phenomenon. Several South American countries, in particular, witnessed temperatures soaring well above the average.

The European Strategic Energy Technology Plan (SET Plan) aims to accelerate the development and deployment of low-carbon technologies, to improve new technologies and to bring down their costs, by facilitating the funding of projects in the energy sector. In the long run, new-generation technologies must be developed through breakthroughs in research to meet the greater ambition of reducing EU greenhouse gas emissions by 80% before 2050. The SET Plan identifies 10 actions for research and innovation. The key action number 1, becoming number 1 in renewables, includes integrating renewable technologies in the energy systems and reducing costs of technologies. Spain chairs the Concentrated Solar Power/Solar Thermal Electricity (CSP/STE) Implementation Plan, whose aim is to significantly reduce the cost of existing technology in the short term and to work towards the development of the next generation technology in the longer term.

CSP plants utilise mirrors to focus the sun's energy, propelling steam turbines that generate electricity. Currently, this technology constitutes a minor fraction of Europe's renewable energy generation, with a global installation of around 5 GW_e, 2.3 GW_e of which is concentrated in Spain. However, its potential for growth is substantial, given CSP's unique ability to deliver renewable electricity on demand, unlike alternative technologies which rely on energy source availability. This dispatchability is made possible through integrated energy storage, allowing plants to respond to peak demands, maintain production during sunlight absence, and offer ancillary services to the grid. As

* Corresponding author.
E-mail address: j.ruiz@umh.es (J. Ruiz).

https://doi.org/10.1016/j.applthermaleng.2024.123718
Received 20 February 2024; Received in revised form 13 June 2024; Accepted 16 June 2024
Available online 21 June 2024

Nomenclature

A	Frontal area (m^2)
a_V	Surface area of exchange per unit of volume (m^2 m^{-3})
c	Constant in ASHRAE correlation
c'	Constant in ASHRAE correlation
c_p	Specific heat (J kg^{-1} K^{-1})
f	Frequency level of the fan (Hz)
h	Enthalpy (J kg^{-1})
h_C	Heat transfer coefficient (W m^{-2} K^{-1})
h_D	Mass transfer coefficient (kg m^{-2} s^{-1})
h_v	Enthalpy of vapour (J kg^{-1})
Le	Lewis factor ($= h_C / \left(h_D c_{p_{ma}}\right)$)
m	Constant in ASHRAE correlation
m'	Constant in ASHRAE correlation
$\dot{m}$	Mass flow rate (kg s^{-1})
Me	Merkel number ($= h_D a_V V / \dot{m}_w$)
N	Number of data points
n	Constant in ASHRAE correlation
Q	Volumetric flow rate of water (m^3 s^{-1})
R^2	R-squared
T	Temperature (K)
T_{wb}	Wet bulb temperature (°C)
V	Volume of the transfer region (m^3)
y_i	Measurement variable for the ith data point
$\hat{y}_i$	Estimated value of variable y_i
$\bar{y}$	Mean value of the experimental values

Greek symbols

ϕ	Relative humidity (%)
ω	Humidity ratio (kg kg^{-1})

Subscripts

a	Air
evap	Evaporated
∞	Ambient conditions
M	Merkel
P	Poppe
s	Saturated
v	Vapour
w	Water
1	Inlet
2	Outlet

Abbreviations

ACC	Air Cooled Condenser
ACHE	Air Cooled Heat Exchanger
ANN	Artificial Neuronal Networks
CCS	Combined Cooling Systems
CSP	Concentrated Solar Power
PSA	Plataforma Solar de Almería
RMSE	Root Mean Square Error
SAM	System Advisor Model
WCT	Wet Cooling Tower

technological leader in this sector, the EU stands to benefit substantially from such expansion. To sustain its global leadership, the European industry must continue to pioneer more advanced and competitive technologies.

The choice of condensation system is crucial for the overall performance of CSP plants. The efficiency of a CSP plant is defined, mainly, by the pressure and the temperature of the steam both entering and leaving the turbine. The steam conditions at the turbine outlet are defined by the temperature at which the steam is condensed.

Wet cooling is usually the preferred option since water-cooled systems' performance relies on the inlet air wet-bulb temperature. Therefore, it involves a lower level in the condensation temperature and a higher thermal efficiency. Palenzuela et al. [1] observed enhancements in the range of 6%–7% when comparing wet-cooled and dry-cooled CSP plants. This study focused on the assessment of various cogenerated CSP plus Desalination plants that integrated different conventional cooling systems. Thus, CSP plants commonly use an evaporation process (often by means of cooling towers) to provide the cooling water source for the condenser. The main drawback is the high water use, which is in the order of 2.3 to 3.5 m^3 h^{-1} per MW_{th}, [2]. According to this prediction, a 50-MW_e power plant running at 35% thermal efficiency will need 214 m^3 h^{-1} or 1.87 million tons per year of water if wet cooling is used to dispose of 93 MW of heat. Due to the fact that the deployment of CSP plants make sense in areas with high radiation levels, where in turn, there is an important water scarcity, the use of cooling systems that reduce the water consumption is of great interest. The Spanish National Integrated Energy and Climate Plan (PNIEC) identifies water as a vulnerable resource at risk for STE production. To mitigate this risk, one of the proposed lines of work in the PNIEC is the study of technological improvements in cooling for dissipating the heat from the thermodynamic cycle.

On the other hand, dry cooling eliminates the water used in steam condensation. Another advantage is to eliminate the plume (mixture of the humid outlet air and the ambient air) since the efficiency of the collectors closer to the dissipation system can be reduced. However, these systems imply a reduced efficiency and a higher cost of electricity in the power plant, which can be around 8% as indicated in the aforementioned reference, [1], especially during periods of high ambient air temperature that frequently match with peak system demand and higher electricity sale prices. This decline in performance occurs because these systems rely on the dry-bulb temperature of the ambient air.

For a CSP power plant, the choice between wet and dry cooling systems involves a number of trade-offs including the availability and cost of water, environmental aspects, and the cost of electric power. Numerous innovative cooling systems hold the potential to significantly reduce water consumption. These include hybrid cooling systems, integrating dry and wet cooling methods into a single device [3–5], and Combined Cooling Systems (CCS) that incorporate separate dry and wet cooling systems. One of the main advantages of CCS is their ability to reject heat through either dry or wet systems, or both, utilising them in series or parallel depending on ambient conditions and plant requirements. When it comes to CCS, various configurations have been proposed. The most frequently cited approach in the literature involves integrating an Air Cooled Condenser (ACC) alongside a Wet Cooling Tower (WCT) [6,7]. In this setup, the steam discharged from the turbine can be condensed either through the ACC or via a surface condenser connected to the WCT. An alternative configuration, as recently proposed by Palenzuela et al. [8], involves a combination of a WCT and an Air-Cooled Heat Exchanger (ACHE) sharing a surface condenser. In this arrangement, the turbine's exhaust steam is condensed through the surface condenser, and the heated cooling water can be cooled either by the WCT or the ACHE. Combined cooling systems stand out as the optimal choice for CSP plants thanks to their potential for water consumption reduction without penalising the power production. It is due to their ability for flexible operation in response to variable

ambient conditions (radiation and temperature). Preliminary studies carried out by several authors of this paper in [9] gave interesting results for a commercial CSP plant (type Andasol-1) integrating a CCS. It was found that a water reduction of up to 50% is possible with this kind of cooling systems compared to the only-wet cooling option, and an increase of 2.5% in the power generation compared to the only-dry cooling option. In this work, black-box models for the dry and wet cooling systems were used using the Thermoflex software.

In the market, several computer software programs can be found that utilise models for the plant components that are black boxes. These models allow little flexibility in terms of changes to either the component selection or the model's internal equations or assumptions. These limitations constitute a challenge when customising or adapting the model according to specific research needs. For example, it poses a real limitation when one component is not included in the software database (i.e. hybrid cooling systems) or when different existing components cannot be used for the same purpose (i.e. dry and wet systems into a combined cooling system), [9]. Other commercial softwares do allow modifying the models of the plant components by acting on the equations that govern their behaviour (i.e TRNSYS or System Advisor Model, SAM). However, the default options usually involve simple models that include several simplifying assumptions in the calculations. For instance, the SAM software uses the latent heat of water evaporation along with the heat rate rejected in the cooling tower to predict the water losses due to evaporation, which is an estimation since part of the heat is transferred by convection. For a precise evaluation of the potential of the combined cooling systems for CSP plants, thorough models of each individual component are needed. In the case of the wet cooling tower, if the equations used by the software do not adequately capture the physics of the problem, the evaluation of the water consumption may not be realistic, and this is a crucial factor in CSP. Precise models for each component of the CCS will allow to develop accurate optimisation tools to evaluate the most effective operational strategies that ensure the needed optimal balance between water and electricity [9]. Likewise, the optimisation tool can be used in the whole plant model (CSP with a CCS) in order to accurately perform annual simulations that allow carrying out comprehensive techno-economic evaluations.

The accurate estimation of the water consumed by the wet cooling system and its performance constitutes the main motivation of this research. Models based on physical equations consider the underlying physics of the heat and mass transfer processes occurring in the exchange area of the tower, and have proven their capability to accurately predict the performance of the tower in the past.

The modelling of wet cooling towers through physical equations traces its origins back to the Merkel theory [10]. This theory, while historically significant, relies on several critical assumptions, including the assumption that the Lewis factor equals 1, that the air exiting the tower is saturated with water vapour, and that the reduction in water flow rate due to evaporation is disregarded in the energy balance. According to Bourillot [11], the Merkel method is easily applicable and provides accurate predictions of cold water temperature when an appropriate coefficient of evaporation is employed. However, the Merkel theory fails in estimating properties related to warm air leaving the fill and calculating changes in water flow rates due to evaporation. These measurements are crucial for estimating water consumption and predicting the behaviour of plumes emitted from the cooling tower. Jaber and Webb [12] developed equations for the direct application of the effectiveness-NTU method to both counterflow and crossflow cooling towers. This approach proved to be especially beneficial in crossflow scenarios, streamlining solutions compared to traditional numerical methods. The effectiveness-NTU method shares the same simplifying assumptions as the Merkel method. Hence, Merkel and effectiveness-NTU theories produce nearly identical results. Poppe and Rögener [13] introduced the Poppe theory, deriving governing equations for heat and mass transfer in wet cooling towers without the simplifying assumptions used in the Merkel method. Kloppers [14] and Kloppers and Kröger [15] extensively compared various prediction methods. Their studies concluded that the Poppe method outperforms the Merkel method, providing a more precise representation of the fundamental physics involved. The Poppe theory accurately predicts the evolution of humid air and computes evaporated water, closely matching the outcomes of comprehensive cooling tower experiments. It also forecasts the moisture content of the outlet air, making it highly recommended for precise analysis when determining outlet air state is essential.

The well-known Merkel number is a dimensionless value widely accepted as the coefficient of performance for a wet cooling tower. This parameter can be used for different purposes, such as cooling tower experimental analysis, simulation or optimisation, [16–18]. The Merkel number is not constant but varies with operating conditions. When plotted against the water-to-air mass flow ratio (i.e., the ratio between water and air mass flow rates flowing inside the cooling tower), it approximates a straight, decreasing line when logarithmic coordinates are used. This variation is often represented as a single curve (correlation) that only depends on the water-to-air mass flow ratio, disregarding the effect of changes in air velocity and the influence of the water mass flow rate on the pressure levels at the spray nozzle.

This paper addresses the comparative evaluation of different theories based on physical equations and correlations to predict the performance and water consumption of a wet cooling tower. Two theories (Poppe and Merkel) as well as three correlations have been considered, compared and discussed in this investigation. The introduction of novel correlations for predicting cooling tower performance stands out as a key innovation in this research.

The paper is structured as follows: Section 2 includes the description of the facility where the experimental tests were conducted, the mathematical modelling and the experimental procedure. Section 3 presents and discusses the main results obtained during this research. Finally, Section 4 summarises the main findings and includes recommendations for future research.

2. Experimental methodology

2.1. Experimental pilot plant

The pilot plant for combined cooling systems is shown in Fig. 1, and it was specifically built for the purpose of this research. The facility is located at Plataforma Solar de Almería (PSA) in Tabernas, Almería, Spain. A detailed description of the plant can be found in Palenzuela et al. [8]. It comprises three different circuits: cooling, exchange, and heating. The experiments presented in this research were conducted in the cooling circuit, Fig. 2, which consists of a combination of a WCT and a ACHE sharing a surface condenser. Here, the refrigeration water flows within the tube bundle of surface condenser and is cooled by either the WCT or the ACHE. Both systems have a designed thermal power of 204 kW_{th}. In this study, the wet-only operational mode was utilised. In this configuration, cooling water (designated as FT-003 in Fig. 1) is pumped from the cooling tower basin to the surface condenser via Pump 1, circulating through Valve 2 in position I up to the entry point of the WCT, where it is sprayed. The airflow velocity within the tower is regulated by a variable frequency drive (SC-001). As the basin level decreases due to evaporation and drift losses, demineralised water (FT-004) is added to replenish the system. Measuring this make-up flow enables the determination of the water consumption of the tower. Refer to Table 1 for specific details about the sensors employed in this operational mode, including their characteristics in terms of uncertainty. Note that the sensors measuring the air velocity, temperature, and relative humidity at the outlet area of the wet cooling tower are not permanently installed in the plant. Portable sensors were used instead in the experiments since the Merkel number calculation requires the mass flow rate of air as an input.

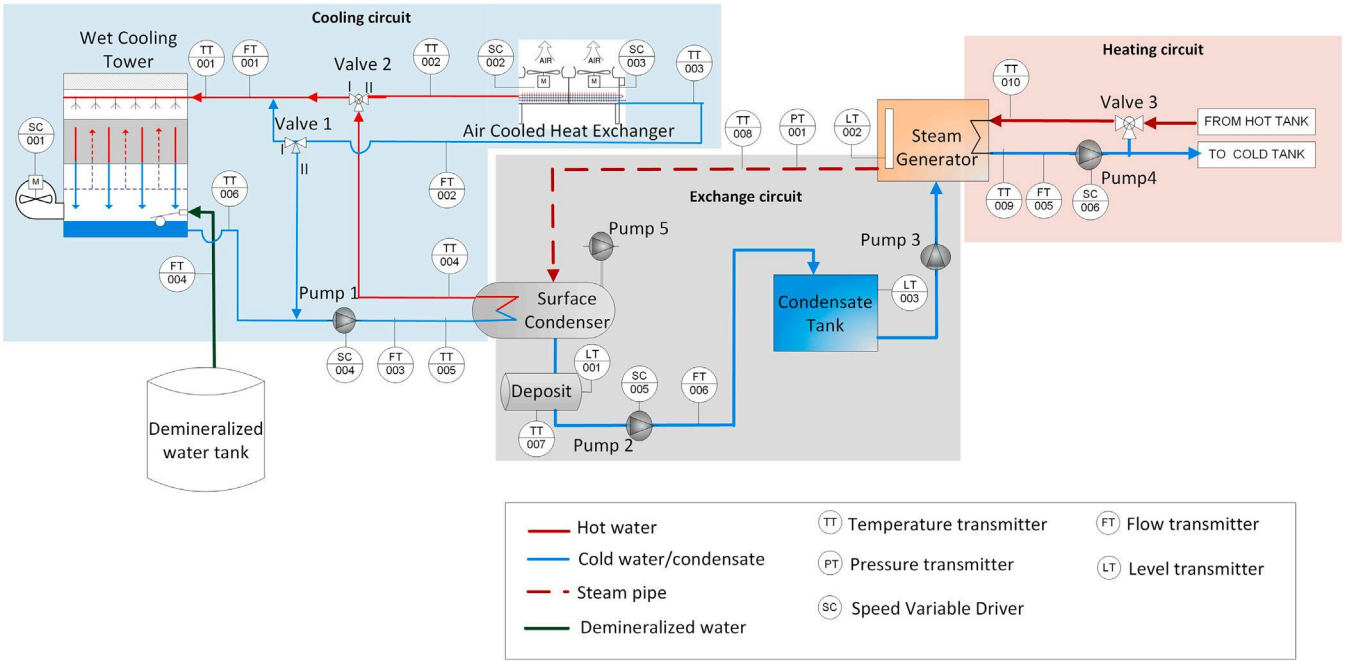

Fig. 1. Diagram illustrating the layout and operation of the combined cooling systems pilot plant at PSA.

Table 1
Sensors specifications ([a] value of the temperature in °C, [b] of reading, [c] full scale).

Variable	Sensor	Range	Uncertainty
Water temperature, TT-001, TT-006	Pt100	0–100 °C	$0.03 + 0.005 \cdot T^{a}$
Cooling water flow rate, FT-001	Vortex flow meter	9.8–25 $m^3\ h^{-1}$	± 0.65% o.r.[b]
Make-up water flow rate, FT-004	Paddle wheel flow meter	0.05–2 $m^3\ h^{-1}$	± 0.5% of F.S[c] + 2.5% o.r
Ambient temperature	Pt1000	−40–60 °C	±0.4@20 °C
Ambient relative humidity	Capacitive sensor	0%–98%	± 3% o.r @20 °C
Air velocity	Impeller anemometer	0.1–15 $m\ s^{-1}$	$\pm 0.1 m\ s^{-1}$ + 1.5% o.r
Outlet air temperature	Pt100	−20–70 °C	±0.5 °C
Outlet air humidity	Capacitive sensor	0–100%	± 2%

2.2. Mathematical modelling

2.2.1. Merkel and Poppe theories

The Merkel number (Eq. (1)) is a dimensionless quantity used in the analysis of heat and mass transfer in various engineering applications. It is particularly important in the context of wet cooling towers, since it quantifies the complex mass transfer processes taking place within the exchange area of the tower [15,19–21].

$$\mathrm{Me} = \frac{h_D A}{\dot{m}_w} = \frac{h_D a_v V}{\dot{m}_w}. \tag{1}$$

As previously stated in Section 1, the computation of the Merkel number can be done using two main established theories for evaluating cooling tower performance: the Merkel and Poppe methods. The Merkel number evaluated using the Merkel theory, Me_M, can be calculated as shown in Eq. (2). If the water inlet temperature, water outlet temperature, air inlet dry-bulb temperature, air inlet wet-bulb temperature, water mass flow rate and airflow rate are known, this equation is solvable. However, the integral evaluation does not have a direct mathematical solution. Instead, numerical integration techniques are necessary to evaluate the integral accurately. The four-point Chebyshev integration technique is recommended by several internationals standards [22,23] to determine Me_M. If two intervals are used in conjunction with the trapezoidal rule, the integral, or Merkel number, is given by the right-hand side of Eq. (2).

$$\mathrm{Me}_M = \frac{h_D A}{\dot{m}_w} = \frac{h_D a_v V}{\dot{m}_w} = \int_{T_{w_2}}^{T_{w_1}} \frac{c_{p_w}}{h_{s_w} - h} dT_w \approx c_{p_w} \frac{(T_{w_1} - T_{w_2})}{4} \sum_{j=1}^{4} \frac{1}{(h_{s_w} - h)_j}. \tag{2}$$

Within the Poppe theory, the authors derived governing equations for heat and mass transfer in the transfer region of the cooling tower. Hence, this theory is generally favoured for its more comprehensive approach. According to the Poppe theory, the major following equations for the heat and mass transfer are obtained:

$$\frac{d\omega}{dT_w} = \frac{c_{p_w} \frac{\dot{m}_w}{\dot{m}_a} \left(\omega_{s_w} - \omega\right)}{\left(h_{s_w} - h\right) + (\mathrm{Le} - 1)\left[\left(h_{s_w} - h\right) - \left(\omega_{s_w} - \omega\right) h_v\right] - \left(\omega_{s_w} - \omega\right) h_w}, \tag{3}$$

$$\frac{dh}{dT_w} = c_{p_w} \frac{\dot{m}_w}{\dot{m}_a} \left[1 + \frac{\left(\omega_{s_w} - \omega\right) c_{p_w} T_w}{\left(h_{s_w} - h\right) + (\mathrm{Le} - 1)\left[\left(h_{s_w} - h\right) - \left(\omega_{s_w} - \omega\right) h_v\right] - \left(\omega_{s_w} - \omega\right) h_w}\right], \tag{4}$$

$$\frac{d\,\mathrm{Me}_P}{dT_w} = \frac{c_{p_w}}{\left(h_{s_w} - h\right) + (\mathrm{Le} - 1)\left[\left(h_{s_w} - h\right) - \left(\omega_{s_w} - \omega\right) h_v\right] - \left(\omega_{s_w} - \omega\right) h_w}. \tag{5}$$

The quantity referred to as Me_P in Eq. (5), is the Merkel number based on the Poppe theory. The detailed derivation process and simplification of the governing equations of the Poppe theory, as well as the solving procedure using the fourth order Runge–Kutta method, can be found in [14,24].

2.2.2. Correlations for the Merkel number

As mentioned in Section 1, it is well established that, in wet cooling towers, the Merkel number is not a constant value. Instead, it varies depending on the operating conditions. Traditionally, the Merkel number corresponding to different operating conditions can be correlated in terms of the water-to-air mass flow ratio, as in Eq. (6). This is the

(a) Top view of the cooling circuit.

(b) Forced mechanical draft wet cooling tower.

Fig. 2. Cooling circuit in combined cooling systems pilot plant at PSA.

prevalent approach in the literature, [18,24–26]. However, as indicated in ASHRAE [27], this expression is derived by neglecting the influence of air velocity. When this effect is accounted for, the correlation of Me can be expressed according to the family of curves shown in Eq. (7), which can be mathematically simplified until obtaining the rightmost side of the equation. Few authors have used this equation to represent the transfer characteristic (Merkel number) [25,28,29]. Finally, a novel correlation has been introduced in this work (Eq. (8)) to account for the effect of the water mass flow rate on the spray characteristics of the nozzle. When $\dot{m}_w$ increases, the pressure level in the nozzles increases as well. This necessarily changes the size and velocity of the sprayed droplets, which directly impacts on the term a_v in Eq. (1). The Merkel number and the constants c and n will change accordingly. In this sense, correlations for constants c and n as a function of $\dot{m}_w$ were developed to overcome the limitation of the traditional correlation, Eq. (6).

$$\mathrm{Me} = c\left(\frac{\dot{m}_w}{\dot{m}_a}\right)^{-n}, \tag{6}$$

$$\mathrm{Me} = c\left(\frac{\dot{m}_w}{\dot{m}_a}\right)^{-n} {v_a}^m = c'\ \dot{m}_w^{-n'}\ \dot{m}_a^{m'}, \tag{7}$$

$$\mathrm{Me} = c\left(\frac{\dot{m}_w}{\dot{m}_a}\right)^{-n}, \quad c = f(\dot{m}_w) \quad \text{and} \quad n = f(\dot{m}_w). \tag{8}$$

2.3. Experimental procedure

In this study, a comprehensive analysis was conducted through 16 sets of experiments to assess the thermal performance of the cooling tower. As previously mentioned, the Merkel number depends on the operating conditions (water and air mass flow rates). Pump 1 in Fig. 1 was used to vary $\dot{m}_w$, while the modifications to $\dot{m}_a$ were made using the fan frequency designated as SC-001 in the same figure. Both variables were adjusted within the permissible operational limits of the plant. In the case of the water flow, it ranged from 8 to 24 $m^3\ h^{-1}$. The air mass flow rate was modified by changing the frequency from 12.5 Hz to a maximum of 50 Hz. As a result, the experimental water-to-air mass flow ratio values ranged from 0.5 to 5. In all conducted tests, the thermal load remained approximately constant at 170 kW_{th}.

To ensure stable conditions during the tests, the standards UNE 13741, titled “Thermal Performance Acceptance Testing of Mechanical Draught Series Wet Cooling Towers” [30], and CTI’s “Acceptance Test Code for Water Cooling Towers” [23], were adopted as benchmarks. These standards specify the test duration and the allowed variations of the most representative ambient and operating magnitudes (water flow rate, heat load, cooling tower range, wet-bulb and dry-bulb temperatures and wind velocity) during the tests.

The sequence for the experimental procedure is schematically depicted in Fig. 3. Once the test runs are performed, the experimental dataset is used to calculate the Merkel number employing both, the Merkel and Poppe theories described in Section 2.2.1. Afterwards, constants in Eqs. (6)–(8) are obtained by fitting the experimental data for the calculated Merkel number. With the aid of the six sets of correlations developed (2 theories and 3 correlations), the following variables are predicted in order to assess the goodness of the theory-correlation combination: the outlet water temperature (T_{w_2}), the outlet air temperature (T_{a_2}) and the tower water consumption ($\dot{m}_{w_{\mathrm{evap}}}$). The effectiveness of the models in approximating the experimental data is evaluated through the calculation of the R-squared (R^2) and the Root Mean Square Error (RMSE). The statistical coefficient R-squared (R^2) [31] quantifies the extent to which the variance in the predicted variable can be accounted for by the independent variable in a regression model. An ideal fit is denoted by a value of 1, indicating that the model’s predictions perfectly align with the observed data. The calculation of R^2 is presented in Eq. (9), where $\bar{y}$ represents the average of the observed experimental data and $\hat{y}_i$ is the estimated value for the same variable. The parameter N represents the total count of available data.

$$R^2 = 1 - \frac{\sum_{i=1}^{N}(y_i - \hat{y}_i)^2}{\sum_{i=1}^{N}(y_i - \bar{y})^2}. \tag{9}$$

RMSE is a statistical indicator of the disparities between the model-predicted values and the actual observed values. Mathematically, it is computed as the square root of the mean of the squared deviations between the predicted and observed values, as in Eq. (10).

$$\mathrm{RMSE} = \sqrt{\frac{1}{N}\sum_{i=1}^{N}(y_i - \hat{y}_i)^2}. \tag{10}$$

2.4. Uncertainty analysis

An uncertainty analysis was made according to the method proposed by the ISO Guide [32]. A Type B evaluation of standard uncertainty (u) was conducted using the sensor specifications listed in Table 1. The combined standard uncertainty was calculated using the uncertainty propagation command of the Engineering Equation Solver

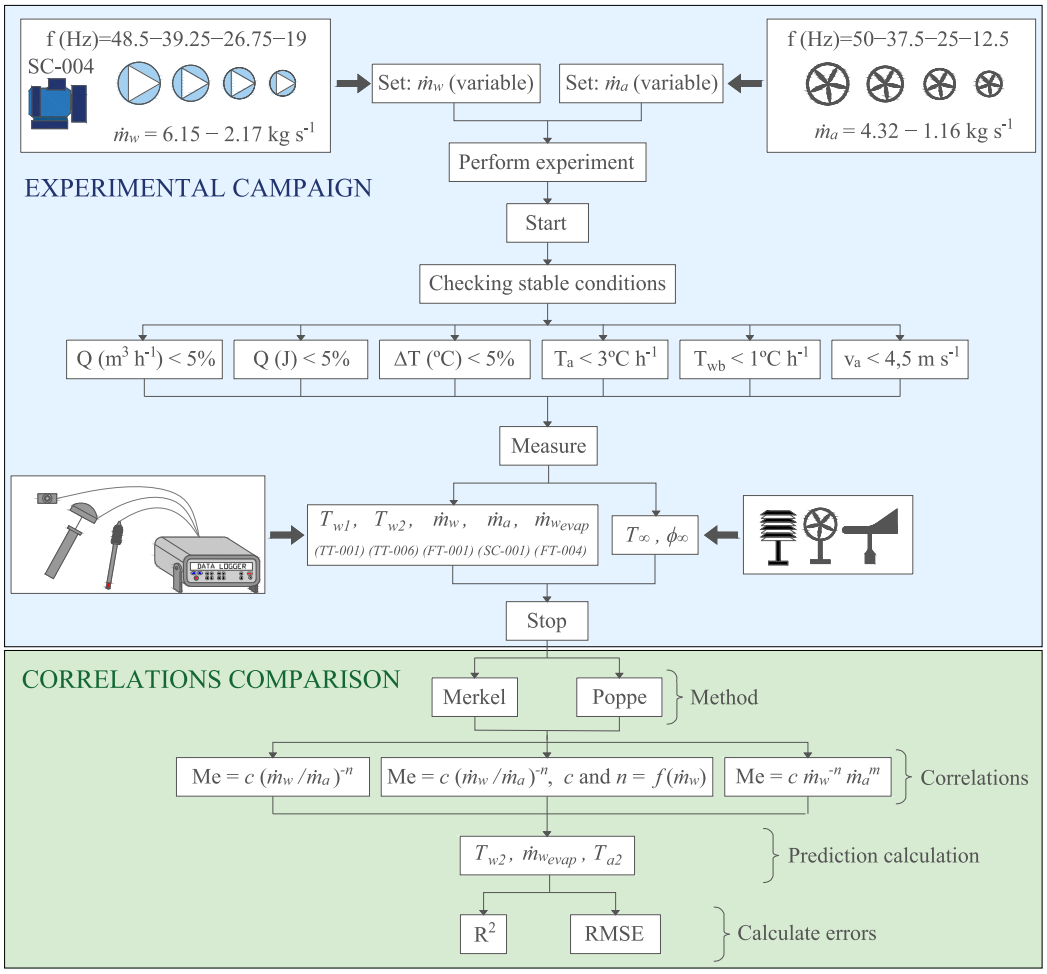

Fig. 3. Scheme of the experimental procedure and model development and evaluation.

(EES), based on the well-known law of uncertainty propagation:

$$u_c = \sqrt{\sum_{i=1}^{N} \left(\frac{\partial f}{\partial x_i} \right)^2 + u^2(x_i)}, \tag{11}$$

where u_c is the combined uncertainty of each key performance indicator, $u(x_i)$ are the standard uncertainties of the variables or measurements on which the indicator depends, and $\partial f / \partial x_i$ are often referred to as the sensitivity coefficients of these variables. Finally, the expanded uncertainty is computed by multiplying the combined uncertainty by a coverage factor k. coverage factor of $k = 1.645$ was considered, ensuring a 90%-level-of-confidence intervals. The results of this uncertainty analysis for the key performance indicators (Merkel number and water-to-air mass flow ratio) are shown in Section 3.

3. Results and discussion

This section presents the results of the 16 experimental tests outlined in Section 2.3. Table 2 contains the average values for all the magnitudes registered during the tests and used for the Merkel number computation, encompassing environmental and tower operational conditions. All the tests were conducted during summer. Hence, the observed variations of the ambient temperature (T_∞), which ranged from 32.84 °C to 40.50 °C, and relative humidity (ϕ_∞), that spanned from 12.97% to 39.58%. The experimental values of the water mass flow rate ($\dot{m}_w$) were 2.17–6.15 kg s^{-1} and the mass flow rate of air ($\dot{m}_a$) ranged between 1.16 and 4.32 kg s^{-1}. Accordingly, the following range of water-to-air mass flow ratios was covered: $0.511 \leq \dot{m}_w/\dot{m}_a \leq 5.13$. Additionally, two key output magnitudes are included in the table: outlet air temperature (T_{a_2}) and the water lost by evaporation ($\dot{m}_{w_{evap}}$). Both variables are measured in the tests, but they are not used in either the Merkel or Poppe theories to calculate the Merkel number for a particular test run. However, they are used along T_{w_2} for assessing the performance of the theories and correlations compared in the paper.

The calculated Merkel number for the Merkel and Poppe theories as a function of the water-to-air mass flow ratio is shown in Fig. 4. The decreasing Me for increasing $\dot{m}_w/\dot{m}_a$ trend observed in this figure, has been extensively reported in the literature [16,18,24–26], and it is explained due to the increase in the amount of water per unit of air leading to a less effective cooling [26]. The relationship between Me and $\dot{m}_w/\dot{m}_a$ follows a linear pattern when plotted on a log–log scale. This involves that, as the ratio $\dot{m}_w/\dot{m}_a$ increases, its impact on Me becomes less significant. This behaviour is attributed to the decrease in the fraction of water that evaporates per unit of inlet water with increasing $\dot{m}_w/\dot{m}_a$ values. When $\dot{m}_w/\dot{m}_a$ reaches its minimum, it indicates the maximum air flow rate achievable for a given water flow rate to be cooled. This scenario maximises the driving force and, thus, the Merkel number. Conversely, as $\dot{m}_a$ decreases gradually, the driving force diminishes for a given $\dot{m}_w$, leading to a decrease in Me. The experimental expanded uncertainty of the results is included in this figure. The mean values for the Me and $\dot{m}_w/\dot{m}_a$ expanded uncertainties, calculated following the procedure indicated in Section 2.4, are 11% and 6.49%, respectively. These values correspond to the calculated values for the Merkel theory. No significant variations were observed for the corresponding uncertainties obtained with the Poppe theory.

Table 2
Summary of the average main ambient and operation magnitudes registered during the experimental test runs.

Test	Q (m^3 h^{-1})	f (Hz)	T_∞ (°C)	ϕ_∞ (%)	T_{wb_∞} (°C)	T_{w_1} (°C)	T_{w_2} (°C)	T_{a_2} (°C)	$\dot{m}_a$ (kg s^{-1})	$\dot{m}_w$ (kg s^{-1})	$\dot{m}_{w_{evap}}$ (kg s^{-1})
1	≈8	12.5	33.31	39.58	22.53	48.88	34.79	46.32	1.193	2.173	0.050
2		25	34.60	30.41	21.34	44.64	27.97	38.04	2.623	2.170	0.066
3		37.5	34.11	38.58	22.92	44.43	26.51	34.73	3.666	2.169	0.069
4		50	36.02	29.94	22.23	43.74	25.43	34.97	4.248	2.170	0.091
5	≈12	12.5	40.50	13.11	19.97	46.85	36.94	49.64	1.157	3.263	0.058
6		25	39.75	12.97	19.50	40.30	28.42	39.92	2.588	3.272	0.075
7		37.5	36.93	22.39	20.79	38.13	26.25	35.51	3.648	3.266	0.097
8		50	35.79	16.13	18.24	35.34	23.32	32.33	4.319	3.268	0.087
9	≈18	12.5	34.69	32.55	21.94	46.53	39.44	47.83	1.177	4.895	0.058
10		25	33.57	27.24	19.83	38.37	30.15	38.25	2.619	4.914	0.071
11		37.5	35.66	25.14	20.71	35.39	27.57	35.94	3.637	4.942	0.075
12		50	33.53	29.29	20.30	34.50	26.27	33.36	4.292	4.940	0.086
13	≈24	12.5	32.84	38.77	21.99	46.25	40.57	46.99	1.186	6.096	0.057
14		25	34.25	16.50	17.42	36.41	29.81	39.49	2.596	6.127	0.072
15		37.5	35.99	16.91	18.59	33.54	27.04	35.38	3.651	6.133	0.078
16		50	35.80	14.73	17.83	31.30	24.87	32.99	4.302	6.147	0.085

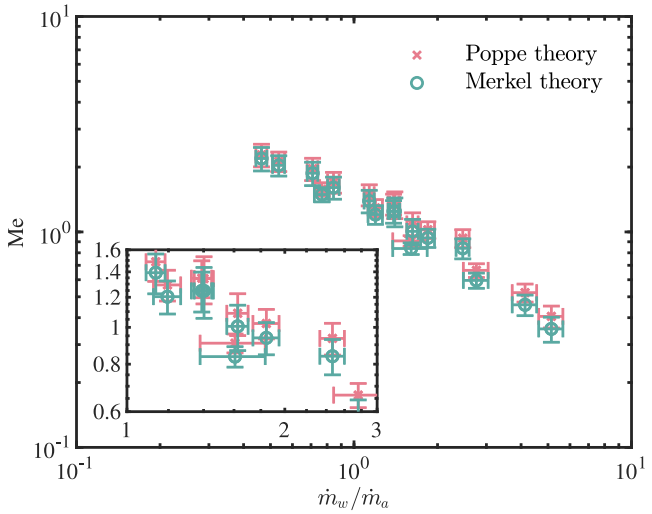

Fig. 4. Experimental Merkel number a function of $\dot{m}_w/\dot{m}_a$ calculated using the Poppe and Merkel theories.

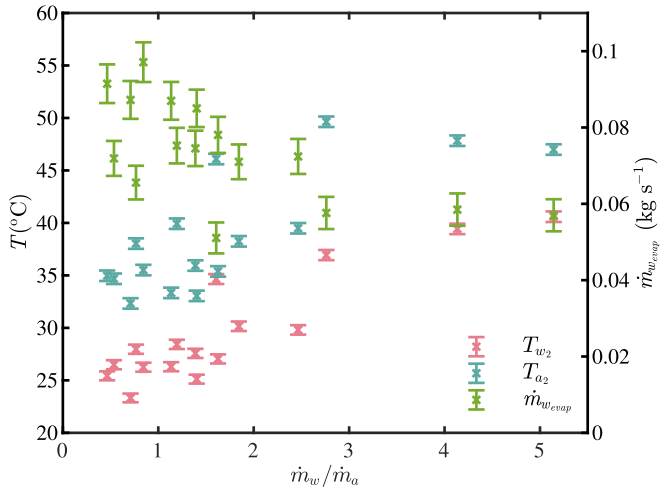

Fig. 5. Experimental results for $\dot{m}_{w_{evap}}$, T_{a_2} and T_{w_2} as a function of $\dot{m}_w/\dot{m}_a$.

Fig. 5 illustrates the variation of the three key output magnitudes used for comparative purposes (T_{w_2}, T_{a_2} and $\dot{m}_{w_{evap}}$) with the water-to-air mass flow ratio. For convenience and better understanding, a dual y-axis chart is used because of the different orders of magnitude observed for the different plotted variables. The error bars for each variable, obtained employing the sensor information (standard uncertainty) displayed in Table 1, are included in the figure.

Concerning the water lost due evaporation, the general trend observed is that $\dot{m}_{w_{evap}}$ decreases with $\dot{m}_w/\dot{m}_a$, which can also be interpreted as an increase in the evaporation rate when $\dot{m}_a$ gets larger for a given $\dot{m}_w$. An increase in $\dot{m}_a$ for a given $\dot{m}_w$ increases the driving force for evaporation. The different levels observed for T_{a_2} depend on the air mass flow rate. If the heat rate to be dissipated is kept constant, higher air temperatures will be obtained for the lower $\dot{m}_a$ levels. The air temperatures rose during the experiments up to 50 °C for the low frequency-levels test runs. Finally, an increase with $\dot{m}_w/\dot{m}_a$ is observed in the outlet water temperature, T_{w_2}. This behaviour is attributed to the decrease in the Merkel number with increasing $\dot{m}_w/\dot{m}_a$ values.

3.1. Influence of the theory (Merkel and Poppe)

The influence of the theory used to calculate the Merkel number can be discussed using the results depicted in Fig. 4. Taking as a reference the results provided by the Poppe theory, since they are the most rigorous, it can be observed that the Merkel theory underestimates the Merkel number calculation ($\mathrm{Me}_P > \mathrm{Me}_M$). This fact can be explained because of the simplifying assumptions inherent to the Merkel theory. These results are aligned with several bibliographic studies that had previously reported the Poppe theory overestimating the Merkel number predicted by the Merkel theory [14,24,33]. The average difference, obtained by averaging the difference for each water-to-air mass flow ratio, is 7.63%, and slightly increases with $\dot{m}_w/\dot{m}_a$ from 3.89% for $\dot{m}_w/\dot{m}_a = 0.511$ to 12.53% for $\dot{m}_w/\dot{m}_a = 5.13$.

3.2. Influence of the correlation

As explained in Section 2.2.2, it is common practice to use the ratio of water-to-air mass flow as the independent variable when deriving a correlation for the Merkel number of a wet cooling tower. This is usually represented by an equation of the form $\mathrm{Me} = c\,(\dot{m}_w/\dot{m}_a)^{-n}$. However, this is not the only approach. This correlation neglects the influence of modifying $\dot{m}_w$ on spray pressure and subsequently on spray characteristics and evaporation. Therefore, in this study, this factor has been taken into account by introducing a function of $\dot{m}_w$ to determine the values of c and n. Finally, this work also incorporates the correlation proposed by ASHRAE [27], described by an equation of the form $\mathrm{Me} = c'\,\dot{m}_w^{-n'}\,\dot{m}_a^{m'}$, which considers the values of $\dot{m}_w$ and $\dot{m}_a$ independently. Constants included in the previous equations are presented in Table 3.

The coefficients for the correlation $\dot{m}_w/\dot{m}_a$ were obtained by performing a power-law fit of the data of Me as a function of $\dot{m}_w/\dot{m}_a$

Table 3
Constants for the different combinations correlation-theory used.

Correlation	Theory	$c - c'$	$n - n'$	m'
$\dot{m}_w/\dot{m}_a$	Poppe	1.5655	0.6720	–
	Merkel	1.4683	0.7075	–
c and $n = f(\dot{m}_w)$	Poppe	$0.0929\dot{m}_w + 1.2838$	$0.0441\dot{m}_w + 0.6322$	–
	Merkel	$0.0897\dot{m}_w + 1.1963$	$0.0453\dot{m}_w + 0.6717$	–
$\dot{m}_w$ and $\dot{m}_a$	Poppe	1.2445	0.5888	0.7830
	Merkel	1.1567	0.6228	0.8245

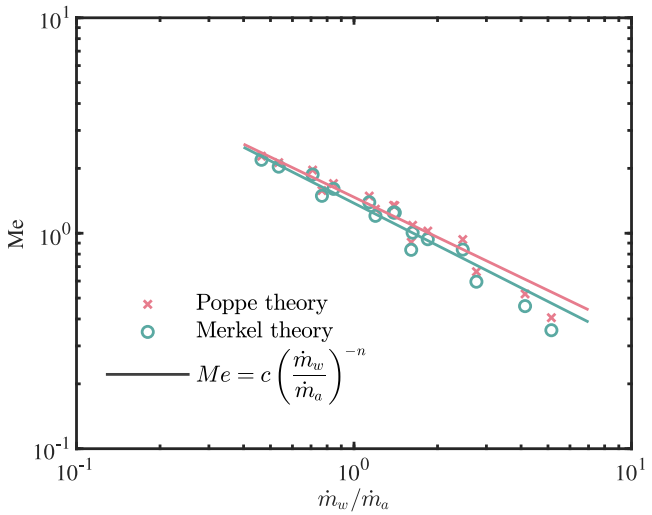

Fig. 6. Experimental and correlated results for the Merkel number as a function of $\dot{m}_w/\dot{m}_a$ calculated using the Poppe and Merkel theories. Correlation $\dot{m}_w/\dot{m}_a$, Eq. (6).

(linear trend on logarithmic scale). Fig. 6 illustrates the experimental data presented in Fig. 4 where the predictions of the $\dot{m}_w/\dot{m}_a$ correlation are overlapped with the experimental values.

Regarding the correlation involving the coefficients c and n as a function of $\dot{m}_w$, these parameters were derived through a similar process, a power-law fit using the data of $\dot{m}_w/\dot{m}_a$ and Me. However, this fitting was conducted for each distinct level of $\dot{m}_w$, leading to the derivation of four sets of values for c and n. Subsequently, these values were subjected to linear regression, resulting in an equation of the form presented in Table 3. The fits are presented in Fig. 7 for the Poppe (Fig. 7(a)) and Merkel (Fig. 7(b)) theories.

Finally, for the $\dot{m}_w$ and $\dot{m}_a$ correlation, the experimental data was fitted to an equation of the form described in Eq. (7), and the parameters c, n, and m were determined. This process yields a linear trend on the logarithmic scale, similar to the previous cases. However, in this instance, separate linear fits can be obtained for each level of $\dot{m}_w$ and $\dot{m}_a$ examined, resulting in different lines on the logarithmic plots. Figs. 8 and 9 illustrate the overlay of the results predicted by the correlations with experimental data. The legend accompanying these plots show the mean values of mass flow rate of water and air of the four tests conducted. When investigating the influence of water flow rate on the Merkel number, a distinct trend in Me becomes evident for different levels of $\dot{m}_w$ (as seen in Fig. 8). This behaviour arises from the changes in nozzle pressure levels due to variations in water mass flow rate, influencing the physical configuration of sprayed droplets and, consequently, the heat exchange surface (term a_v, Eq. (1)) and, thus, Me. This trend is observable in both theories and has not been previously documented in the reviewed literature. Similar patterns were observed for different $\dot{m}_a$ levels (Fig. 9). Altering the air velocity affects the mass transfer coefficient (h_D term, Eq. (1)), accounting for the distinct behaviours observed at the same $\dot{m}_w/\dot{m}_a$ level.

3.3. Comparative evaluation of the proposed theory-correlation combinations

In order to determine the theory-correlation combination that provides the best results, the predictions of each combination were compared to the experimental results. The different sets of equations derived in the previous section enabled the prediction of T_{w_2}, T_{a_2} and $\dot{m}_{w_{\text{evap}}}$, which are presented in Fig. 10. The solid line in this figure represents the perfect agreement between the predictions and the observed values. This figure also includes the experimental uncertainty of the compared magnitude. Table 4 includes the maximum and average experimental-predicted differences for the previously-mentioned variables. Additionally, the reliability of the collected data was further assessed using statistical techniques, as mentioned in Section 2.3. The calculated values for the Root Mean Square Error (RMSE) and R-squared (R^2) are presented in Table 5.

At first glance, it is evident that the two analysed theories and the three considered correlations predict the outlet water temperature with remarkable accuracy. This fact can be seen in Fig. 10(a). The maximum deviation for all the theory-correlation combinations is less than 1 °C, which is found for the Merkel theory and the $\dot{m}_w/\dot{m}_a$ correlation. In general, the Merkel theory predictions are slightly worse than the Poppe theory's one. Concerning correlations, the standard correlation ($\dot{m}_w/\dot{m}_a$ in this paper, Eq. (6)) is the least accurate one, which translates into R^2 = 0.9918 and RMSE = 0.4650. The order of the correlations performing best to worst is: c and $n = f(\dot{m}_w) \approx \dot{m}_w$ and $\dot{m}_a > \dot{m}_w/\dot{m}_a$ (Eq. (8) ≈ Eq. (7) >Eq. (6)). In the light of this, it can be assessed that the use of any of the correlations considered in this paper along the Poppe or Merkel theories accurately predict the outlet water temperature of the cooling tower.

Furthermore, one of the main advantages of the Poppe theory is its ability to forecast the evolution of warm, moist air in the transfer area (fill) of the cooling tower. This capability allows predicting the conditions of the air leaving the tower and, consequently, the amount of water lost due to evaporation. This fact is of utmost importance in the performance evaluation of a wet cooling tower operating in a CSP plant. The choice of the dissipation system may depend on water availability, making this prediction crucial. The Merkel theory, on the other hand, assumes that the air leaves the tower saturated, only characterised by its enthalpy (obtained from the energy balance). This fact explains why there are no predictions for T_{a_2} and $\dot{m}_{w_{\text{evap}}}$ with the Merkel theory in Tables 4 and 5.

Fig. 10(b) presents the comparison of the computed and experimental water consumption results for all tests. As it can be seen, the Poppe model predicts the amount of evaporated water with reasonable accuracy, within the uncertainty levels of the measuring instrumentation used. However, it is observed that the model consistently underpredicts the experimental results for all the tests. It is important to note that the model calculates the water lost through evaporation. In a cooling tower there are other water losses such as drift losses, blowdown and other minor losses (splash, leaks, overflow, etc.). Hence, it makes sense that the model forecasts are lower than the experimental results. For example, assuming a drift emissions rate of 0.05%, as reported by [34] for a lath-type drift eliminator, the predictions would roughly match the measured results. However, the predictions for four tests show significant discrepancies (test runs 4, 7, 8 and 12 in Table 2). These tests mainly correspond to those with higher fan frequency levels. One possible explanation could be that the relative contribution of centrifugal and drag forces on the droplets, can lead to scenarios where an increase in the air flow velocity, increases the amount of drift emissions, as explained in Ruiz et al. [34]. Also, a more plausible explanation could be related to droplet breakthrough or re-entrainment of water droplets. This phenomenon occurs when the air velocity is high, leading to the suction of water out of the drift eliminators. The water then becomes re-entrained into the exiting airstream. Those losses are not accounted

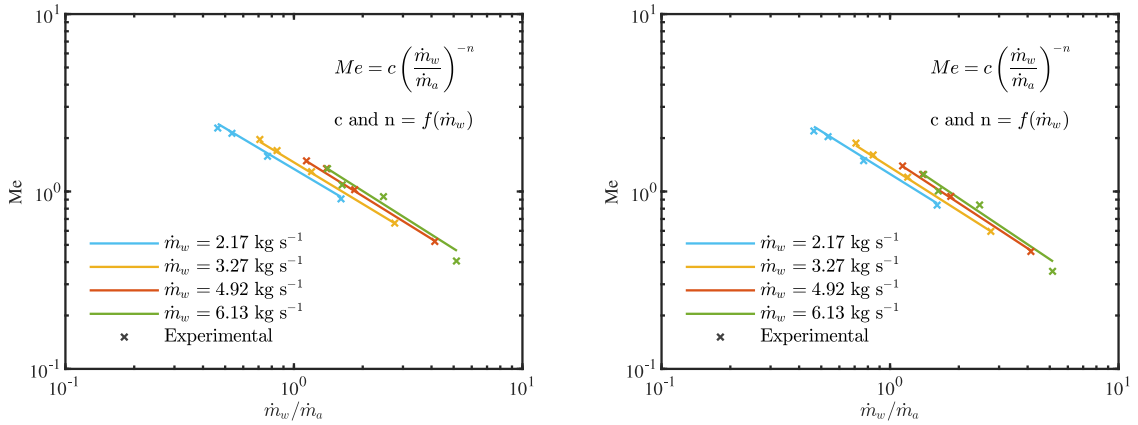

(a) Poppe theory. (b) Merkel theory.

Fig. 7. Experimental and correlated results for the Merkel number as a function of $\dot{m}_w/\dot{m}_a$ calculated using the Poppe and Merkel theories. Correlation with c and $n = f(\dot{m}_w)$, Eq. (8).

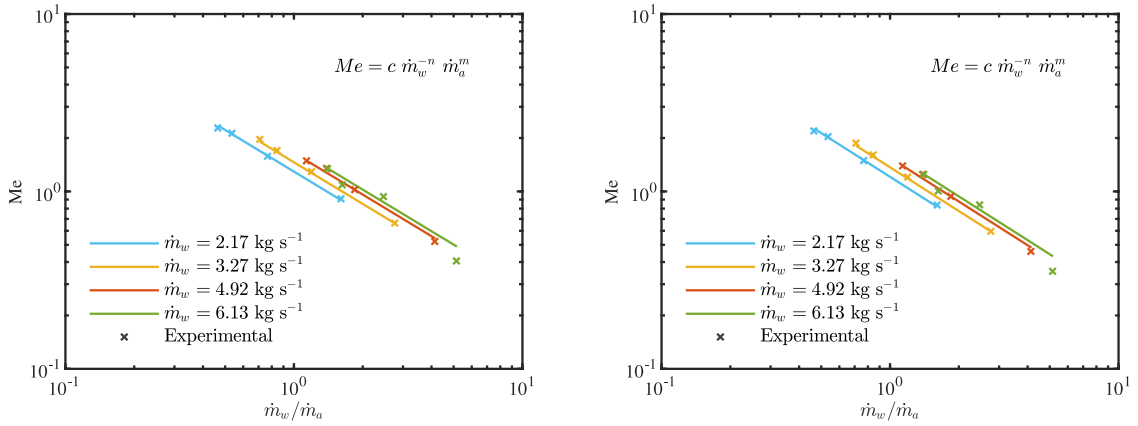

(a) Poppe theory. (b) Merkel theory.

Fig. 8. Experimental and correlated results for the Merkel number as a function of $\dot{m}_w/\dot{m}_a$ calculated using the Poppe and Merkel theories. $\dot{m}_w$ and $\dot{m}_a$ correlation, Eq. (7). Water mass flow rate levels.

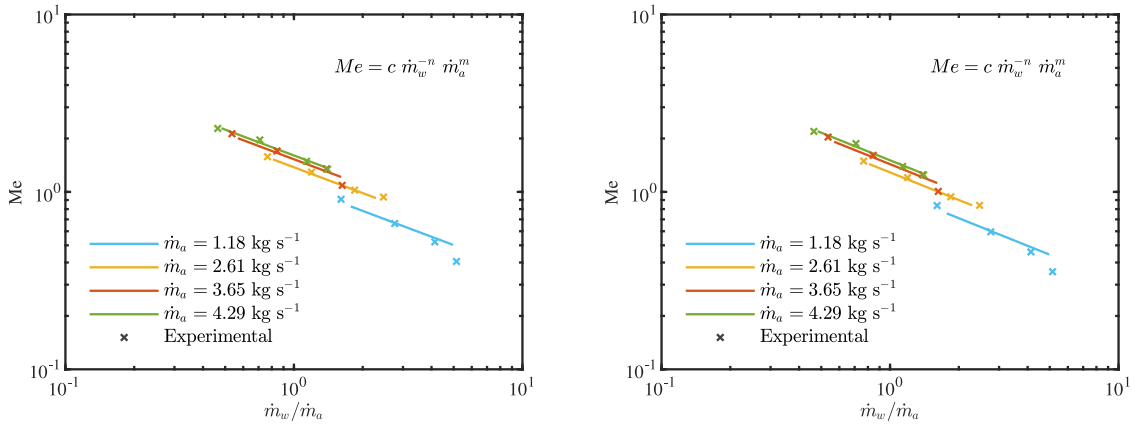

(a) Poppe theory. (b) Merkel theory.

Fig. 9. Experimental and correlated results for the Merkel number as a function of $\dot{m}_w/\dot{m}_a$ calculated using the Poppe and Merkel theories. $\dot{m}_w$ and $\dot{m}_a$ correlation, Eq. (7). Air mass flow rate levels.

for in the model, but have an impact on the measured make-up water. Both hypotheses are consistent with the observed results. It should be noted that no significant variations for this magnitude were observed between the correlations compared.

Fig. 10(c) compares the temperature of the air leaving the cooling tower. Again, the Poppe model demonstrates a high degree of accuracy in its predictions. The results obtained from the 16 conducted tests exhibit an average deviation of 6.78% (equivalent to 2.45 °C, as

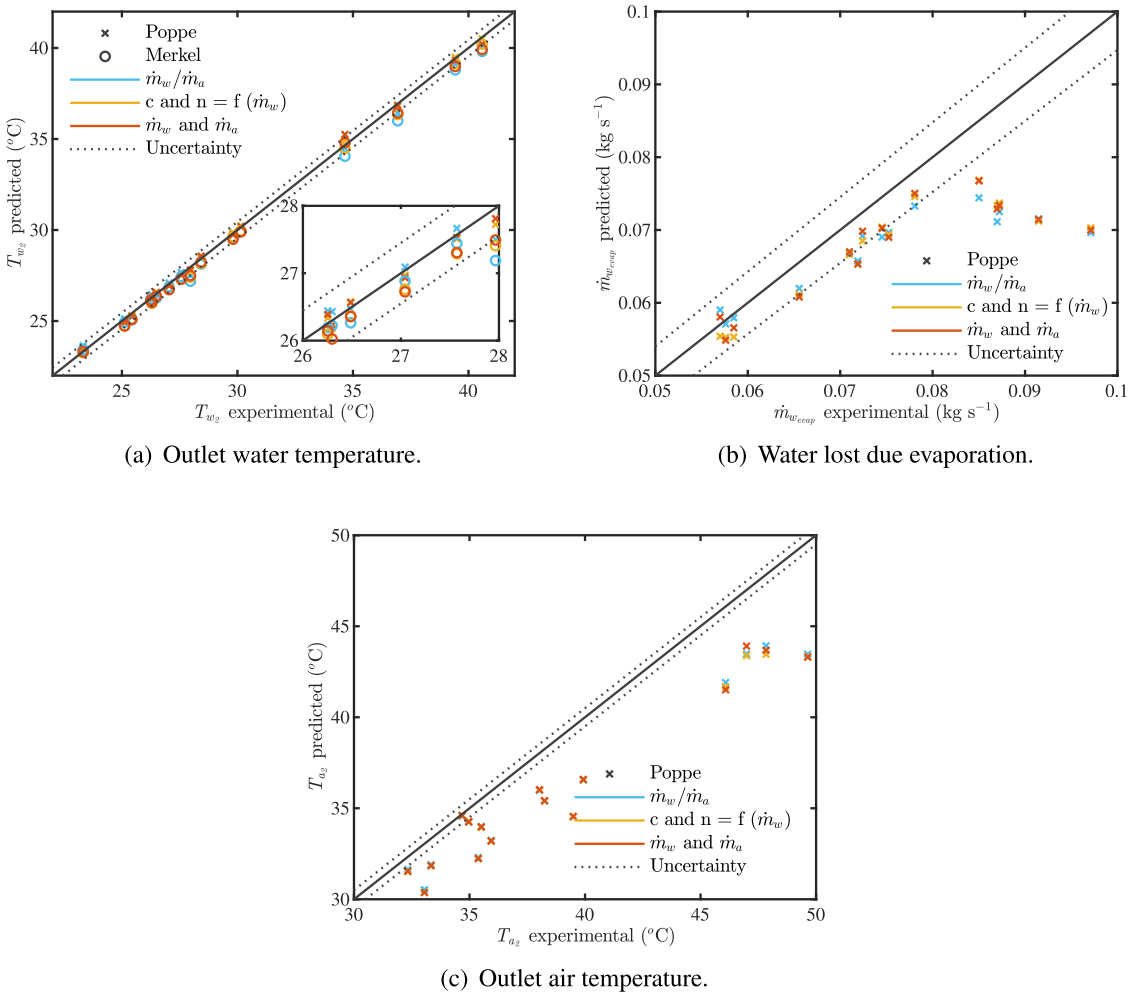

(a) Outlet water temperature.

(b) Water lost due evaporation.

(c) Outlet air temperature.

Fig. 10. Comparison between experimental and predicted cooling tower (a) outlet water temperature, (b) water consumption and (c) outlet air temperature.

Table 4
Averaged and maximum differences between experimental and predicted results for the theory-correlation combinations analysed in this paper concerning T_{w_2}, T_{a_2} and $\dot{m}_{w_{evap}}$.

Correlation	Theory	T_{w_2}		$\dot{m}_{w_{evap}}$		T_{a_2}	
		Aver.dif. (°C)	Max.dif. (°C)	Aver.dif. (kg s^{-1})	Max.dif. (kg s^{-1})	Aver.dif. (°C)	Max.dif. (°C)
$\dot{m}_w/\dot{m}_a$	Poppe	0.21	0.50	0.01	0.03	2.75	6.17
	Merkel	0.36	0.94	–	–	–	–
c and $n = f(\dot{m}_w)$	Poppe	0.10	0.24	0.01	0.03	2.83	6.31
	Merkel	0.27	0.59	–	–	–	–
$\dot{m}_w$ and $\dot{m}_a$	Poppe	0.14	0.46	0.01	0.03	2.79	6.33
	Merkel	0.28	0.64	–	–	–	–

Table 5
Calculated values for RMSE and R^2 for the theory-correlation combinations analysed in this paper concerning T_{w_2}, T_{a_2} and $\dot{m}_{w_{evap}}$.

Correlation	Theory	T_{w_2} (°C)		$\dot{m}_{w_{evap}}$ (kg s^{-1})		T_{a_2} (°C)	
		R^2	RMSE	R^2	RMSE	R^2	RMSE
$\dot{m}_w/\dot{m}_a$	Poppe	0.9974	0.2648	0.3299	0.0108	0.6716	3.1793
	Merkel	0.9918	0.4650	–	–	–	–
c and $n = f(\dot{m}_w)$	Poppe	0.9995	0.1113	0.3838	0.0103	0.6510	3.2774
	Merkel	0.9965	0.3061	–	–	–	–
$\dot{m}_w$ and $\dot{m}_a$	Poppe	0.9988	0.1787	0.3744	0.0104	0.6595	3.2370
	Merkel	0.9960	0.3268	–	–	–	–

presented in Table 4) for the best correlation ($\dot{m}_w/\dot{m}_a$). These results correspond to R^2 values of 0.6716 and an RMSE of 3.1793. Again, no significant variations were observed for the correlations considered in the investigation. These differences are minimal for higher fan frequency values (associated with elevated $\dot{m}_a$ values). As fan frequency decreases, the disparities grow. This phenomenon can be attributed to the reduced uniformity in the distribution of air temperature at the outlet tower area as the fan frequency diminishes. As the experimental values were calculated by averaging the temperature measurements made at a several points (the cooling tower exit area was divided into 9 quadrants and the variables were registered at the centre of each quadrant), a reduced uniformity would lead to higher differences compared to a uniform temperature profile.

Table 6
Calculated values for RMSE and R^2 for the comparative analysis with data available in the literature [24–26].

Study	Correlation	Theory	T_{w_2} (°C)		$\dot{m}_{w_{evap}}$ (kg s^{-1})		T_{a_2} (°C)	
			R^2	RMSE	R^2	RMSE	R^2	RMSE
Navarro et al. [24]	$\dot{m}_w/\dot{m}_a$	Merkel	0.9731	1.0315	–	–	–	–
	$\dot{m}_w$ and $\dot{m}_a$	Merkel	0.9938	0.4969	–	–	–	–
	$\dot{m}_w/\dot{m}_a$	Poppe	0.9739	1.0176	–	–	0.8399	1.1504
	$\dot{m}_w$ and $\dot{m}_a$	Poppe	0.9940	0.4889	–	–	0.8535	0.9447
Lucas et al. [25]	$\dot{m}_w/\dot{m}_a$	Merkel	0.9665	0.4691	–	–	–	–
	$\dot{m}_w$ and $\dot{m}_a$	Merkel	0.9932	0.2118	–	–	–	–
Ruiz et al. [26]	$\dot{m}_w/\dot{m}_a$	Merkel	0.9966	0.0857	–	–	–	–
	$\dot{m}_w$ and $\dot{m}_a$	Merkel	0.9967	0.0843	–	–	–	–
	$\dot{m}_w/\dot{m}_a$	Poppe	0.9967	0.0843	–	–	–	–
	$\dot{m}_w$ and $\dot{m}_a$	Poppe	0.9969	0.0825	–	–	–	–
This study	$\dot{m}_w/\dot{m}_a$	Merkel	0.9918	0.4650	–	–	–	–
	$\dot{m}_w$ and $\dot{m}_a$	Merkel	0.9960	0.3268	–	–	–	–
	c and $n = f(\dot{m}_w)$	Merkel	0.9965	0.3061	–	–	–	–
	$\dot{m}_w/\dot{m}_a$	Poppe	0.9974	0.2648	0.3299	0.0108	0.6716	3.1793
	$\dot{m}_w$ and $\dot{m}_a$	Poppe	0.9988	0.1787	0.3744	0.0104	0.6595	3.2370
	c and $n = f(\dot{m}_w)$	Poppe	0.9995	0.1113	0.3838	0.0103	0.6510	3.2774

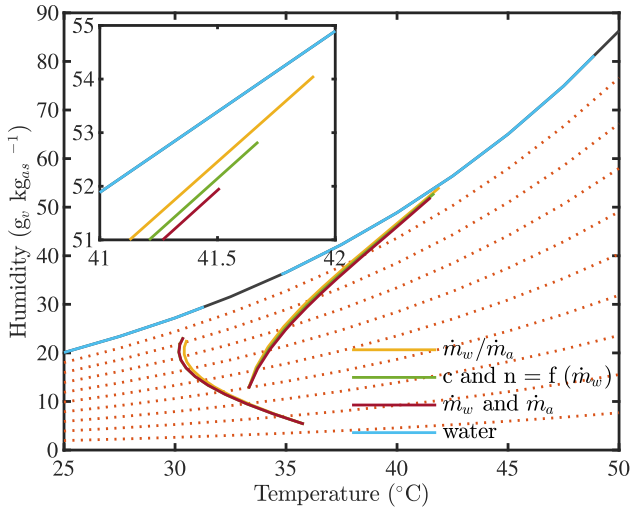

Fig. 11. Evolution of the properties of water and air in a psychrometric chart for test runs 1 (right) and 16 (left), Table 4.

Fig. 11 depicts the evolution of the air properties in the psychrometric chart for two experimental tests (test runs 1 and 16, as detailed in Table 2) calculated with the Poppe theory. These tests correspond to the upper and lower bounds of the intervals for the tested water and air mass flow rates. Since the driving force for the evaporative cooling process is the difference between the air's enthalpy and the enthalpy of saturated air computed at the water's temperature, the evolution of the water temperature is also illustrated as a solid line that overlaps with the saturation curve. The length of the air trajectory is affected by the fan frequency level. Lower frequency levels involve lower air velocities and, therefore, increased interaction time between the air and water.

As expected, the air experiences an increase in moisture content due to water evaporation. However, concerning the temperature evolution, the trend is not that evident. The air temperature tends to reach the water temperature in all exchange sections. Given the counterflow arrangement between the water and air streams, the inlet air exchanges heat and mass with the water at outlet conditions and it shifts until reaching the cooling tower outlet, where the exchange takes place between the air and the water at inlet conditions. This explains the path followed by the air in both cases and, specially, the curved-path observed in test 16 (left-hand side of Fig. 11). An additional observation regarding air and water temperatures involves tests where the air temperature at the cooling tower's inlet section is higher than the water temperature (for example, left-hand side of Fig. 11) at that specific location (outlet area in that case), $T_a > T_w$. This implies that sensible heat transfers from the air to the water while latent (mass) transfer occurs in the other direction, from the water to the air. Nevertheless, the net exchange of enthalpy continues to favour the air, as depicted in Fig. 11. Consequently, this process induces cooling for both the air and water within this particular location. The prediction of the air properties evolution is quite similar for the three correlations tested. No significant discrepancies are observed.

The evolution of the properties cannot be predicted using the Merkel theory because it relies on the assumption that the air leaves the tower saturated and characterised only by the enthalpy calculated according to the energy balance. Therefore, only the air exit conditions but not the evolution could be depicted in the psychrometric chart. This approach does not account for the reduction in water flow rate due to evaporation.

3.4. Comparison of the obtained results with data available in the literature

This section presents a comparative analysis between the outcomes derived from this research and those documented in the existing literature. The comparative analysis was not limited to the theory-correlation combinations; the performance of the tower was also examined and contextualised.

The bibliographic studies [24–26] were used to provide context for the theories and correlations discussed, since some of the theory-correlation combinations described in this paper are also utilised in these studies.

Table 6 provides the computed values for the R^2 and RMSE for the water and air outlet temperatures, as well as water consumption. This evaluation is carried out in cases where the theory is capable of making predictions or when there is experimental data available. In general, it can be said that the results reported in the literature agree with the conclusions reached in previous sections. All the theory-correlation combinations demonstrate good agreement in predicting the values of T_{w_2} when compared to experimental data. The R^2 values are higher than 0.96 in all the cases. Concerning theories, the Poppe theory forecasts better results than the Merkel theory for the water outlet temperature (only variable that is predicted by both theories). Finally, and regarding correlations, the $\dot{m}_w$ and $\dot{m}_a$ correlation outperforms the standard one ($\dot{m}_w/\dot{m}_a$) when they are directly compared. No relevant conclusions can be drawn from the T_{a_2} comparison. Less favourable values for the R^2 and the RMSE indicators are observed when comparing the results obtained in this study to bibliographic results. This has been previously justified due to the fact that, when a data point comparing predicted and experimental values deviates significantly, its

contribution to the RMSE substantially influences the overall model accuracy. The R^2 coefficient is less sensitive to extreme deviations of individual data points, as it evaluates relative variability rather than the absolute magnitude of errors. Nevertheless, this indicator is also affected by the points deviating from the experimental observations.

To contextualise the tower's performance, the results obtained in this study, featuring a cooling tower equipped with a trickle-type fill, were compared with those of other towers reported in the literature. In Lucas et al.'s study [25], the authors employed a cooling tower equipped with fiberglass vertical corrugated plates as fill material. Similarly, Gharagheizi et al. [35] investigated a tower incorporating both vertical corrugated packing (VCP) and horizontal corrugated packing (HCP). Conversely, Ghazani et al. [36] utilised a fill made of thin film Polypropylene PVC packing. Finally, in the works of Ruiz et al. [26] and Navarro et al. [18], the fill material resembled that used in the present study.

The thermal performance of the investigated towers is compared in Fig. 9, where Fig. 9(a) illustrates the comparison of the Merkel number with the correlation $\dot{m}_w/\dot{m}_a$. Curves for the different towers considered have been plotted against constant approach curves.

The cooling tower approach refers to the difference between the cooling tower outlet cold water temperature and the ambient wet-bulb temperature. Consequently, it serves as a reliable indicator of the cooling tower's performance. The constant approach curves were computed considering a design operating conditions of T_{wb} =27 °C and a cooling tower range of 5 °C . These curves offer valuable insights into the tower's performance across varying conditions. Their shape is determined by the ratio of water mass flow rate to air mass flow rate ($\dot{m}_w/\dot{m}_a$). The ideal scenario where the airflow rate is infinite ($\dot{m}_w/\dot{m}_a = 0$), corresponds to the maximum driving force and the minimum required Merkel number. As the air rate decreases, the driving force diminishes, involving an increase in the required Merkel number. The points of intersection between the constant approach curves and the tower performance curves ($\mathrm{Me} = c\left(\dot{m}_w/\dot{m}_a\right)^{-n}$) denote the specific $\dot{m}_w/\dot{m}_a$ values at which the towers will operate.

Regarding the comparison of the Merkel number, it was observed that for all water-to-air mass flow ratios, the studied cooling tower outperforms other cooling towers documented in the literature. This occurs regardless of whether the towers use the same type of fill or a different one. This could be justified by the fact that using optimised fills increases the wetted surface area (higher coefficient a_V of the Merkel number).

While the Merkel number is an effective metric when comparing the performance of wet cooling towers, its use may not always provide clear insight into the energetic implications of different designs. The key parameter for predicting the performance of a system that incorporates a cooling tower for heat removal (such as a power cycle or refrigeration cycle) is the outlet water temperature. Therefore, the outlet water temperatures for the previously cited cooling towers are also predicted for three different levels of $\dot{m}_w/\dot{m}_a$ (0.6, 0.9, and 1.2). Fig. 12(b) illustrates the projected outlet water temperatures for the bibliographic results considered in this section. As an example, with the cooling tower studied and $\dot{m}_w/\dot{m}_a = 0.9$, an approach of approximately 2.4 °C is achieved. This corresponds to a water outlet temperature of approximately 29.4 °C.

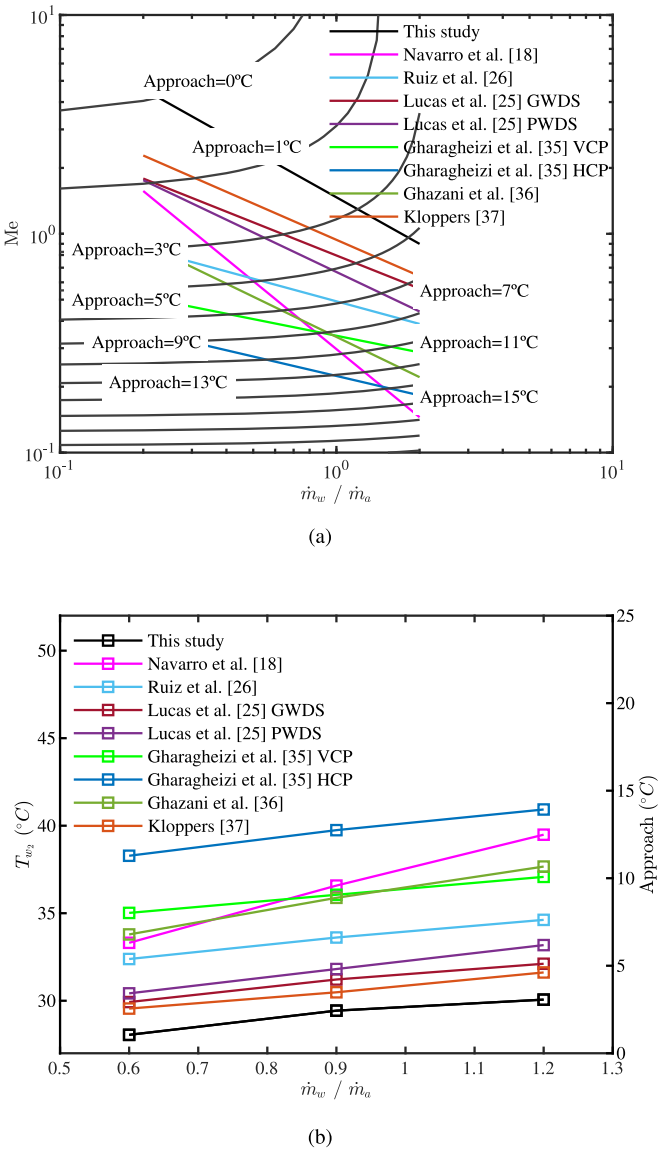

Fig. 12. Comparison between the experimental data obtained in this research and the data reported in the literature [18,25,26,35–37]. (a) Me number and (b) T_{w_2} for the specified conditions.

4. Conclusions and future perspectives

4.1. Conclusions

The primary objective of this research was to model and optimise the operation of integrated combined cooling systems within CSP plants. This study particularly addressed the comparative evaluation of different theories and models based on physical equations to predict the performance of a wet cooling tower. In this sense, the two most popular theories for performance evaluation of wet cooling towers (Poppe and Merkel) as well as three correlations were considered, compared and discussed in this investigation. The introduction of novel correlations for predicting cooling tower performance stood out as a key innovation in this research. The main findings from the research can be summarised as follows:

In view of the results obtained, it can be stated that both theories, Poppe and Merkel, along with the three employed correlations predict, with remarkable accuracy the cooling tower outlet water temperature. The maximum difference found between observed and predicted results was lower than 1 °C (R^2 = 0.9918 and RMSE = 0.4650). Accordingly, if only this magnitude is of interest, the Merkel theory and the standard correlation (Merkel number as a function of the water-to-air mass flow ratio) combination is the most straightforward approach due to its simplicity. However, in CSP plants the prediction of the water consumption is of utmost importance. Therefore, the Merkel theory can be discarded due to its inability to predict the evolution of the air inside the tower exchange area (fill), which enables the calculation of the evaporated water. Hence, the use of the Poppe theory is strongly recommended (if not mandatory) when predicting the performance of

a wet cooling tower operating either independently or as part of a combined system for heat rejection in CSP plants.

The three compared correlations demonstrated similar prediction accuracy. The results indicate that, depending on the studied variable, one correlation performs better than other. For instance, the correlation termed as c and $n = f(\dot{m}_w)$ provides the best T_{w_2} predictions ($R^2 \approx 1$ and RMSE = 0.11°C), the c and $n = f(\dot{m}_w)$ and the $\dot{m}_w$ and $\dot{m}_a$ correlations yield to similar results concerning $\dot{m}_{w_{\text{evap}}}$ calculations ($R^2 \approx 0.38$ and RMSE ≈ 0.01 kg s^{-1}), and the $\dot{m}_w$ and $\dot{m}_a$ correlation showed a closer agreement with the experimental results for T_{a_2}. In order to choose a correlation, the average deviation for all magnitudes was calculated, and it was found that the $\dot{m}_w$ and $\dot{m}_a$ correlation led to the best overall predictions.

Therefore, the combination comprising the Poppe theory and the $\dot{m}_w$ and $\dot{m}_a$ correlation is suggested when evaluating the performance of a wet cooling tower operating in a combined cooling cycle for heat rejection in CSP plants. This combination offer up to 70% better predictions for water temperature and 2% for water consumption, compared to other combinations. The discrepancies found between the proposed approach and the experimental results have been attributed to some physical phenomena not included in the calculation process (drift and re-entrainment) in the case of evaporated water and the non-uniformity of the air temperature profiles at the outlet area of the cooling tower in the case of the outlet air temperature.

Furthermore, the use of a model based on physical equations, such as the combination of the Poppe theory and the correlation suggested in this investigation, presents additional strengths, including the capacity for performance assessment in conditions beyond those directly tested or in scaled systems, provided the system configuration remains consistent. These facts make this combination of theory/model a suitable approach to analyse combined cooling systems in CSP plants.

4.2. Future perspectives

Future investigations must focus on the improvement of the experimental procedure to assess the hypotheses proposed concerning the discrepancies observed for the evaporated water predictions. That involves conducting drift tests to determine the amount of water exiting the tower taken away by the air stream and verifying the temperature distribution in the outlet section of the tower. Also, while the theoretical analysis of the wet cooling tower has demonstrated successful outcomes with moderate complexity, certain variables might benefit from the application of alternative methods available in the literature, for example, black-box models such as artificial neuronal networks (ANN) based on experimental data. This could improve some predictions such as water consumption or reduce model execution time. Ultimately, and in order to achieve the overarching aim of this research (modelling and optimising the combined cooling system), a model for the ACHE should be developed and validated using experimental data from the pilot plant. The WCT and ACHE models can be linked to provide a model for the combined cooling system, which can be eventually used, along the solar field and power block models, to optimise the operation of the plant depending on the environmental conditions and the plant requirements.

CRediT authorship contribution statement

P. Navarro: Writing – review & editing, Writing – original draft, Methodology, Investigation, Formal analysis. **J.M. Serrano:** Writing – original draft, Investigation, Formal analysis. **L. Roca:** Writing – review & editing, Project administration, Funding acquisition, Formal analysis, Conceptualization. **P. Palenzuela:** Writing – review & editing, Project administration, Funding acquisition, Formal analysis, Conceptualization. **M. Lucas:** Writing – review & editing, Methodology, Conceptualization. **J. Ruiz:** Writing – review & editing, Writing – original draft, Supervision, Methodology, Investigation, Formal analysis, Conceptualization.

Declaration of competing interest

The authors declare that they have no known competing financial interests or personal relationships that could have appeared to influence the work reported in this paper.

Data availability

Data will be made available on request.

Acknowledgements

This publication is part of the R&D project PID2021-126452OA-I00, funded by MCIN/AEI/10.13039/501100011033/ and ERDF A way of making Europe. The authors thank the Plataforma Solar de Almería for providing access to its facilities.

References

[1] P. Palenzuela, D.-C. Alarcón-Padilla, G. Zaragoza, Large-scale solar desalination by combination with CSP: Techno-economic analysis of different options for the Mediterranean Sea and the Arabian Gulf, Desalination 366 (2015) 130–138, http://dx.doi.org/10.1016/j.desal.2014.12.037, URL https://www.sciencedirect.com/science/article/pii/S0011916414006845, Energy and Desalination.

[2] A. Cooperman, J. Dieckmann, J. Brodrick, Power plant water use, ASHRAE J. 54 (2012) 65–68.

[3] E. Rezaei, S. Shafiei, A. Abdollahnezhad, Reducing water consumption of an industrial plant cooling unit using hybrid cooling tower, Energy Convers. Manage. 51 (2) (2010) 311–319, http://dx.doi.org/10.1016/j.enconman.2009.09.027.

[4] W. Asvapoositkul, M. Kuansathan, Comparative evaluation of hybrid (dry/wet) cooling tower performance, Appl. Therm. Eng. 71 (1) (2014) 83–93, http://dx.doi.org/10.1016/j.applthermaleng.2014.06.023.

[5] H. Hu, Z. Li, Y. Jiang, X. Du, Thermodynamic characteristics of thermal power plant with hybrid (dry/wet) cooling system, Energy 147 (2018) 729–741, http://dx.doi.org/10.1016/j.energy.2018.01.074.

[6] G. Barigozzi, A. Perdichizzi, S. Ravelli, Wet and dry cooling systems optimization applied to a modern waste-to-energy cogeneration heat and power plant, Appl. Energy 88 (4) (2011) 1366–1376, http://dx.doi.org/10.1016/j.apenergy.2010.09.023.

[7] G. Barigozzi, A. Perdichizzi, S. Ravelli, Performance prediction and optimization of a waste-to-energy cogeneration plant with combined wet and dry cooling system, Appl. Energy 115 (2014) 65–74, http://dx.doi.org/10.1016/j.apenergy.2013.11.024.

[8] P. Palenzuela, L. Roca, F. Asfand, K. Patchigolla, Experimental assessment of a pilot scale hybrid cooling system for water consumption reduction in CSP plants, Energy 242 (2022) 122948, http://dx.doi.org/10.1016/j.energy.2021.122948, URL https://www.sciencedirect.com/science/article/pii/S0360544221031972.

[9] F. Asfand, P. Palenzuela, L. Roca, A. Caron, C.-A. Lemarié, J. Gillard, P. Turner, K. Patchigolla, Thermodynamic performance and water consumption of hybrid cooling system configurations for concentrated solar power plants, Sustainability 12 (11) (2020) http://dx.doi.org/10.3390/su12114739.

[10] F. Merkel, Verdunstungskühlung, VDI Zeitschriff Deutscher Ingenieure, Berlin, Alemania (1925) 123–128.

[11] C. Bourillot, Hypotheses of Calculation of the Water Flow Rate Evaporated in a Wet Cooling Tower, United States, 1983.

[12] H. Jaber, R.L. Webb, Design of cooling towers by the effectiveness-NTU method, J. Heat Transfer 111 (4) (1989) 837–843, http://dx.doi.org/10.1115/1.3250794.

[13] M. Poppe, H. Rögener, Berechnung von rückkühlwerken, VDI wärmeatlas (1991) Mi 1.

[14] J. Kloppers, A Critical Evaluation and Refinement of the Performance Prediction of Wet-Cooling Towers (Ph.D. thesis), University of Stellenbosch, Stellenbosch, South Africa, 2003, URL https://scholar.sun.ac.za/items/49b7c7b4-763c-487a-8ce3-494521816dca.

[15] J. Kloppers, D. Kröger, A critical investigation into the heat and mass transfer analysis of counterflow wet-cooling towers, Int. J. Heat Mass Transfer 48 (3) (2005) 765–777, http://dx.doi.org/10.1016/j.ijheatmasstransfer.2004.09.004, URL https://www.sciencedirect.com/science/article/pii/S0017931004004041.

[16] K. Singh, R. Das, An experimental and multi-objective optimization study of a forced draft cooling tower with different fills, Energy Convers. Manage. 111 (2016) 417–430, http://dx.doi.org/10.1016/j.enconman.2015.12.080, URL https://www.sciencedirect.com/science/article/pii/S0196890416000029.

[17] K. Singh, R. Das, Simultaneous optimization of performance parameters and energy consumption in induced draft cooling towers, Chem. Eng. Res. Des. 123 (2017) 1–13, http://dx.doi.org/10.1016/j.cherd.2017.04.031, URL https://www.sciencedirect.com/science/article/pii/S0263876217302678.

[18] P. Navarro, J. Ruiz, A. Kaiser, M. Lucas, Effect of fill length and distribution system on the thermal performance of an inverted cooling tower, Appl. Therm. Eng. 231 (2023) 120876, http://dx.doi.org/10.1016/j.applthermaleng.2023.120876, URL https://www.sciencedirect.com/science/article/pii/S1359431123009055.

[19] R.K. Singla, K. Singh, R. Das, Tower characteristics correlation and parameter retrieval in wet-cooling tower with expanded wire mesh packing, Appl. Therm. Eng. 96 (2016) 240–249, http://dx.doi.org/10.1016/j.applthermaleng.2015.11.063, URL https://www.sciencedirect.com/science/article/pii/S1359431115013095.

[20] K. Singh, R. Das, A feedback model to predict parameters for controlling the performance of a mechanical draft cooling tower, Appl. Therm. Eng. 105 (2016) 519–530, http://dx.doi.org/10.1016/j.applthermaleng.2016.03.030, URL https://www.sciencedirect.com/science/article/pii/S1359431116303222.

[21] Sanjay, A. Verma, A. Prasad, L. Yadav, A. Yadav, Performance analysis of counter flow cooling tower using reciprocating desiccant mesh, Heat Mass Transf. 56 (2020) 2779–2799, http://dx.doi.org/10.1007/s00231-020-02912-y.

[22] A. Mohiuddin, K. Kant, Knowledge base for the systematic design of wet cooling towers. Part I: Selection and tower characteristics, Int. J. Refrig. 19 (1) (1996) 43–51, http://dx.doi.org/10.1016/0140-7007(95)00059-3, URL https://www.sciencedirect.com/science/article/pii/0140700795000593.

[23] CTI, Code Tower, Standard Specifications. Acceptance Test Code for Water Cooling Towers, Cooling Technology Institute, 2000.

[24] P. Navarro, J. Ruiz, M. Hernández, A. Kaiser, M. Lucas, Critical evaluation of the thermal performance analysis of a new cooling tower prototype, Appl. Therm. Eng. 213 (2022) 118719, http://dx.doi.org/10.1016/j.applthermaleng.2022.118719.

[25] M. Lucas, J. Ruiz, P.J. Martínez, A.S. Kaiser, A. Viedma, B. Zamora, Experimental study on the performance of a mechanical cooling tower fitted with different types of water distribution systems and drift eliminators, Appl. Therm. Eng. 50 (1) (2013) 282–292, http://dx.doi.org/10.1016/j.applthermaleng.2012.06.030, URL https://www.sciencedirect.com/science/article/abs/pii/S1359431112004516.

[26] J. Ruiz, P. Navarro, M. Hernández, M. Lucas, A. Kaiser, Thermal performance and emissions analysis of a new cooling tower prototype, Appl. Therm. Eng. (2022) 118065, http://dx.doi.org/10.1016/j.applthermaleng.2022.118065, URL https://www.sciencedirect.com/science/article/pii/S135943112200031X.

[27] Ashrae, HVAC systems and equipment, in: Chapter 36 Cooling Towers, 2004.

[28] N. Milosavljevic, P. Heikkilä, A comprehensive approach to cooling tower design, Appl. Therm. Eng. 21 (9) (2001) 899–915, http://dx.doi.org/10.1016/S1359-4311(00)00078-8, URL https://www.sciencedirect.com/science/article/pii/S1359431100000788.

[29] J. Kloppers, D. Kröger, Refinement of the transfer characteristic correlation of wet-cooling tower fills, Heat Transf. Eng. 26 (4) (2005) 035–041, http://dx.doi.org/10.1080/01457630590916266.

[30] UNE, Thermal Performance Acceptance Testing of Mechanical Draught Series Wet Cooling Towers, UNE, 2004.

[31] D. Chicco, M.J. Warrens, G. Jurman, The coefficient of determination R-squared is more informative than SMAPE, MAE, MAPE, MSE and RMSE in regression analysis evaluation, PeerJ Comput. Sci. 7 (2021) e623.

[32] J.C. for Guides in Metrology (JCGM), Evaluation of measurement data. Guide to the expression of uncertainty in measurement, 2008.

[33] J.C. Kloppers, D.G. Kröger, Cooling Tower Performance Evaluation: Merkel, Poppe, and e-NTU Methods of Analysis, J. Eng. Gas Turbines Power 127 (1) (2005) 1–7, http://dx.doi.org/10.1115/1.1787504.

[34] J. Ruiz, A. Kaiser, M. Lucas, Experimental determination of drift and PM10 cooling tower emissions: Influence of components and operating conditions, Environ. Pollut. 230 (2017) 422–431, http://dx.doi.org/10.1016/j.envpol.2017.06.073, URL https://www.sciencedirect.com/science/article/pii/S026974911731120X.

[35] F. Gharagheizi, R. Hayati, S. Fatemi, Experimental study on the performance of mechanical cooling tower with two types of film packing, Energy Convers. Manage. 48 (2007) 277–280.

[36] M.A. Ghazani, A.H. ol Hosseini, M.D. Emami, A comprehensive analysis of a laboratory scale counter flow wet cooling tower using the first and the second laws of thermodynamics, Appl. Therm. Eng. 125 (2017) 1389–1401, URL http://www.sciencedirect.com/science/article/pii/S1359431116345203.

[37] J. Kloppers, D. Kröger, Refinement of the transfer characteristic correlation of wet-cooling tower fills, Heat Transf. Eng. 26 (4) (2005) 035–041, http://dx.doi.org/10.1080/01457630590916266.